Local divergence and curvature divergence in first order optics

Cosmas Mafusire & Tjaart P. J. Krüger
Department of Physics, Faculty of Natural and Agricultural Sciences, University of Pretoria, Private Bag X20, Hatfield, 0028, South Africa
Corresponding Author: *cosmasmafusire@gmail.com*

Abstract

The far-field divergence of a light beam propagating through a first order optical system is presented as a square root of the sum of the squares of the local divergence and the curvature divergence. The local divergence is defined as the ratio of the beam parameter product to the beam width whilst the curvature divergence is a ratio of the space-angular moment also to the beam width. It is established that the beam's focusing parameter can be defined as a ratio of the local divergence to the curvature divergence. The relationships between the two divergences and other second moment-based beam parameters are presented. Their various mathematical properties are presented such as their evolution through first order systems. The efficacy of the model in the analysis of high power continuous wave laser-based welding systems is briefly discussed..

1. Introduction

There are three parameters of non-spherical non-Gaussian beams that can be calculated directly from the field distribution at each selected plane [1,2]. These are the beam width, which is the variance of the transversal position, the far-field divergence, which is the variance of the transversal spatial frequency, and the space-angular moment being the covariance of the product of the transversal position and spatial frequency. This moment approach has also been used to characterize beams carrying aberrations [3-5]. The results has shown that closed form solutions of the moments showing their dependence on Zernike aberrations can be easily calculated. The approach has been used to demonstrate how aberrations can influence the focal length of a lens [5]. Once these three parameters are known, other parameters such as the waist location, waist size and Rayleigh range can be derived from the three moments. For this reason, they are the basic parameters that need to be calculated first before the other parameters are to be calculated to completely define a laser beam propagating through a first order system. If the propagation channel is free of aberrations, then the free space first order propagation of these basic parameters through an $ABCD$ system can be expressed using some basic laws involving $ABCD$ matrices; the same laws that can be used to describe the propagation of the derived parameters [1,2]. This implies that the transformations of the basic parameters through the system can be used to derive the corresponding propagation of the derived parameters.

In first order beam propagation, a certain combination of the basic and derived parameters can be used to create the, so-called, propagation invariants whose values do not change throughout the propagation path, provided that no aberrations are generated anywhere in the propagation channel [1,2]. The main parameter is called the beam propagation parameter (BPP), which is directly proportional to the beam quality factor [2]. A typical example is the product of waist width and far-field divergence, which is used as a standard definition for the beam quality factor [6]. The model that is of importance in this paper includes the focusing parameter [7], defined as a value that facilitates the location of the geometric focus of a system. It has the same form as the reciprocal of the Gaussian Fresnel number.

In this paper, we investigate far-field divergence by splitting its square into a sum of the squares of the local divergence and the curvature divergence. We demonstrate that the focusing parameter can be presented as a ratio of local to curvature divergence. We also show how the focusing parameter relates to other beam parameters. In the following section the transformation laws of the second order moments of non-spherical non-Gaussian laser beams through a simple astigmatic first order system are presented. In Section 3, local and curvature divergence, the focusing parameter as well as the free space propagation of their normalized versions are introduced. The results are then applied to first order beam propagation in Section 4. In Section 5, the paper is discussed.

2. Beam parameters and their transformation in first order optics

A general representation of the system is based on how most optical setups are achieved, which is a source-target system that is broken into three main sections: a laser source, processing optics, and the target half space. In this paper, a laser transmission system is proposed, which is comprised of the laser source and the processing optics. The basis of the design is that the laser source produces a beam with fixed output size, divergence and space-angular moments because these properties are set during manufacture. The process optics are a diffraction-limited $ABCD$ system responsible for processing the beam in that it allows the manipulation of the moments to produce the respective required moments for a particular application. As shown in Fig. 1, the source produces a laser beam defined by the three initial moments at plane P, the beam width ω_i, space-angular moment, $V_i = \omega_i^2/R_i$, and far-field divergence, θ_{0i}, where R_i is the field average radius of curvature. The $ABCD$ system converts the source beam into one that has the respective moments, ω, $V = \omega^2/R$, and far-field divergence, θ_0, at $z = 0$, indicated by Q. Thereafter, the beam undergoes free propagation through a space of uniform refractive index in which we place the target at a distance z from the process optics. This half space ($z \geq 0$) is the space after the $ABCD$ system where diagnosis of the system takes place. Therefore, the $ABCD$ matrix for the entire length of this model consists of the elements,

$$\begin{pmatrix}1 & z\\ 0 & 1\end{pmatrix}\begin{pmatrix}A & B\\ C & D\end{pmatrix}=\begin{pmatrix}A+Cz & B+Dz\\ C & D\end{pmatrix}. \tag{1}$$

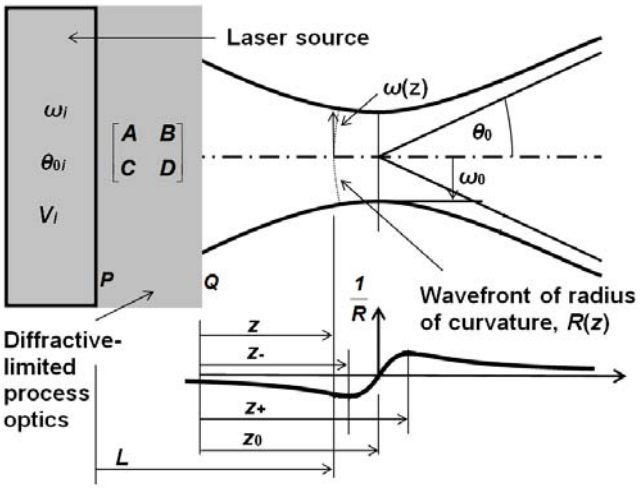

Fig. 1 A laser transmitter in grey consisting of a laser source and diffractive-limited *ABCD* process optics, with the respective source and intermediate parameters as shown. Observation is carried out in the half-space, $z \geq 0$, where the beam experiences free propagation.

The respective moments at the target become $\omega(z)$ and $V(z) = \omega^2(z)/R(z)$. Obviously, the far-field divergence, θ_0, remains the same throughout this path. The focused version of the output beam has a waist of width ω_0 located at a distance z_0 from *Q*. The planes at z_- and z_+ are where the beam's curvature $1/R(z)$ reaches its local minima and maxima, respectively. The depth of focus (also called the confocal parameter) of a laser beam during *ABCD* propagation is defined as $z_+ - z_-$. We will refer to z_- and z_+ as the Rayleigh planes.

a. Beam moments in first order optics

In one dimension, the transformation of these basic moments through the *ABCD* system has been evaluated and found to obey the following equations: [1,2]

$$\omega^2(z) = (A+Cz)^2\omega_i^2 + 2(A+Cz)(B+Dz)V_i + (B+Dz)^2\theta_{0i}^2 \tag{2}$$
$$\theta_0^2 = C^2\omega_i^2 + 2CDV_i + D^2\theta_{0i}^2 \tag{3}$$
$$V(z) = (A+Cz)C\omega_i^2 + (\{A+Cz\}D + \{B+Dz\}C)V_i + (B+Dz)D\theta_{0i}^2 \tag{4}$$

After some manipulation, Eqs. (2) and (3) can be written in terms of the far-field divergence as follows:

$$\omega^2(z) = \omega^2 + 2Vz + \theta_0^2 z^2 \tag{5}$$
$$V(z) = V + \theta_0^2 z, \tag{6}$$

where ω and V are respective moments at point Y corresponding to $z = 0$. These equations can be used to verify that the beam propagation parameter (BPP), usually defined as $2M^2/k$, stays constant throughout the propagation path with k being the laser radiation wave constant. Its square is given by $\omega^2(z)\theta_0^2 - V^2(z)$ at any plane where $z \geq 0$. This result is identical to $\omega_i^2\theta_{0i}^2 - V_i^2$ and $\omega^2\theta_0^2 - V^2$ on the condition that $AD - BC = 1$. Dividing Eq. (2) into Eq. (4) or Eqs. (5) into (6) gives the expression for the evolution of the field curvature: [1,2]

$$\frac{1}{R(z)} = \frac{V(z)}{\omega^2(z)}. \tag{7}$$

The BPP squared calculated at a plane other than the waist can also be defined as $\omega^2(z)\theta_0^2$, from which $V^2(z)$ is removed. This value is directly proportional to the curvature, $1/R(z)$ and creates an artificial waist at which the beam characterization procedure will fulfil the conditions set by the ISO 11146 standard [6]. As stated earlier, the BPP squared value is also given by $(2M^2/k)^2$, which implies that if $\omega(z)$, θ_0 and $V(z)$ are measured at some plane z, M^2 can be easily calculated. As a result, this method is referred to as the curvature-removal method in which the M^2 measurement is carried out in one plane [8].

b. Derived beam parameters in terms of the far-field divergence

Consider the situation whereby the beam converges to a waist such that the curvature becomes positive after the waist. Let us say the waist is located at $z = z_0$. The location of the waist is then found by equating the left hand sides of both Eqs. (4), (6) or (7) to 0, making z_0 the subject and is found to be

$$z_0 = -\frac{V}{\theta_0^2}. \tag{8}$$

Therefore, the waist location can be expressed as a ratio of the space-angular moment to the square of the far-field divergence. To get the waist width, ω_0, we replace z with z_0, as defined by substituting Eq. (8) into Eqs. (2) or (5) with the definition $\omega_0 = \omega(z_0)$ and then rearrange the result by expressing it in terms of BPP to get

$$\omega_0 = \frac{2M^2}{k\theta_0}. \tag{9}$$

From this equation it can be inferred that $\omega_0\theta_0$ is a propagation invariant as mentioned in the introduction. To find the Rayleigh planes, Eq. (7) is differentiated with respect to z, with the result equated to zero leading to the expression

$$z_\pm = \frac{-kV \pm 2M^2}{k\theta_0^2} = z_0 \pm z_R \tag{10}$$

giving us z_- and z_+. It is apparent that the Eq. (10) consists of the sum of two terms, namely the waist location as defined by Eq. (8), and an extra term. The latter term is referred to as the Rayleigh range, z_R, which is half the confocal parameter and defined as,

$$z_R = \tfrac{1}{2}(z_+ - z_-) = \frac{2M^2}{k\theta_0^2}. \tag{11}$$

We can see that $z_R\theta_0^2$ is also a propagation invariant. If we equate it to $\omega_0\theta_0$, another definition of the invariant, we get $\omega_0 = z_R\theta_0$. If we eliminate θ_0 from Eq. (9) as defined by this equation, another variation of the propagation invariant, ω_0^2/z_R is realised.

3. Local and curvature divergence, and the focusing parameter

The BPP at the target can be defined as $\omega^2(z)\theta_l^2(z)$, where $\theta_l(z)$ are the local divergences. It has been specified earlier that the square of this version of the BPP can also be given by $\omega^2(z)\theta_0^2 - V^2(z)$. Comparing the two expressions, the local divergence squared, $\theta_l^2(z)$, is then found to be

$$\theta_l(z) = \left(\theta_0^2 - \frac{V^2(z)}{\omega^2(z)}\right)^{1/2} = \frac{2M^2}{k\omega(z)}. \tag{12}$$

In the limit of large z this parameter tends to 0. At the same time, it can be verified by using Eq. (8) that $\theta_l(z_0) = \theta_0$. At this stage, we propose a new type of divergence which we will to refer to as the curvature divergence, $\theta_c(z)$, defined as

$$\theta_c(z) = \frac{V(z)}{\omega(z)} = \frac{\omega(z)}{R(z)}. \tag{13}$$

We derive the name from fact that this method involves the curvature-removal procedure mentioned earlier. Note that the last term in Eq. (13) originates from using Eq. (7). In the limit of large z, in the far-field, $\theta_c(z)$ converges to θ_0. At the waist, $\theta_c(z_0) = 0$. The two divergences can then be related to each other through the expression,

$$\theta_l^2(z) + \theta_c^2(z) = \theta_0^2. \tag{14}$$

At the Rayleigh planes ($z = z_\pm$), the local and curvature divergences are equal and are both 70.7% of the far-field divergence, $\theta_l(z_\pm) = \theta_c(z_\pm) = \frac{1}{\sqrt{2}}\theta_0$.

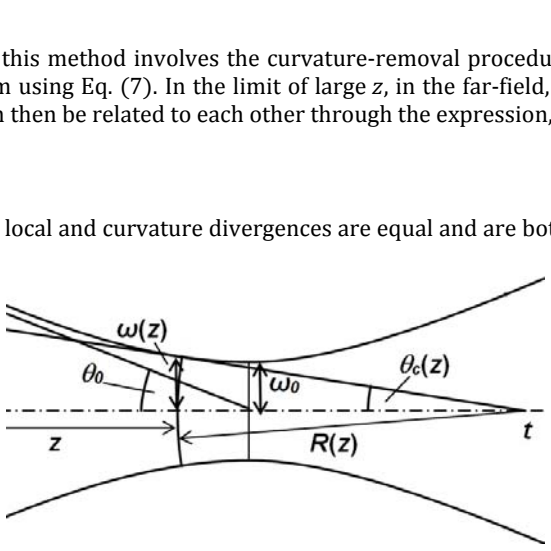

Fig. 2 The curvature divergence, $\omega(z)/R(z)$, subtended by the plane of size $\omega(z)$, and radius of curvature $R(z)$. In comparison, the far-field divergence is subtended by the far-field.

We can now examine the meaning of the curvature divergence utilizing its definition given by the last term in Eq. (13). It is an angle subtended by the curvature of the local field. The angle, $\theta_c(z)$, subtends an arc of radius $R(z)$ with the centre of radius of curvature centred at point t, as illustrated in Fig. 2, which shows the caustic of a beam including the plane of minimum beam size, the waist. If the position of the initial plane is located very far from the waist, the wavefront would have a radius centred at the waist, thus called the far-field divergence, i.e., $\theta_c(z) = \theta_0$. If the initial plane is at the waist, then $\theta_c(z) = 0$ since the curvature of the field would be zero. In between these two extremes, $\theta_c(z)$ is between 0 and θ_0.

a. The focusing parameter

We now present a model based on the focusing parameter using a different derivation from that used in Ref. [7]. Since $\omega_0^2\theta_0^2 = \omega^2(z)\theta_0^2 - V^2(z)$, after making θ_0^2 the subject and rearranging, results in the expression

$$\theta_0^2 = \frac{V^2(z)}{\omega^2(z)}\left(1 + \frac{\omega_0^2}{\omega^2(z) - \omega_0^2}\right). \tag{15}$$

The numerator and denominator of the fraction inside the bracket is then multiplied by θ_0^2 such that the BPP squared waist width in the numerator is replaced by $(2M^2/k)^2$, whilst that in denominator is replaced by $\omega^2(z)\theta_0^2 - V^2(z)$, leading to the result,

$$\frac{\omega_0^2}{\omega^2(z) - \omega_0^2} = \left(\frac{2M^2}{kV(z)}\right)^2. \tag{16}$$

The divergence squared can be expressed as shown by the second term in the following equation:

$$\theta_0^2 = \theta_c^2(z)(1 + N^2(z)) = \theta_l^2(z)(1 + N^{-2}(z)), \tag{17}$$

where $\theta_c(z)$ has been defined in Eq. (13) and $N(z)$ is the focusing parameter given by

$$N(z) = \frac{2M^2}{kV(z)} = \frac{\theta_l(z)}{\theta_c(z)}. \tag{18}$$

The third term of Eq. (17) is a result of replacing $\theta_c^2(z)$ with $\theta_0^2 - \theta_l^2(z)$. Note that the third term in Eq. (18) can be derived from the second equation of Eq. (17). From Eq. (17) we note that $\theta_l(z) = \theta_c(z)$ when $N(z) = \pm 1$, and that when $N(z) = 0$, $\theta_c(z) = \theta_0$ and $\theta_l(z) = 0$, a situation which reverses when $N(z) \to \infty$. Note that from the above derivation, it is obvious that

$$\theta_0^2 = \theta_c^2(1 + N^2) = \theta_l^2(1 + N^{-2}) \tag{19}$$

if the derivation is carried out with $\omega^2\theta_0^2 - V^2$ instead, where N is the focusing parameter at $z = 0$.

Using an alternative version of the propagation invariant given in Eq. (18) means that $N(z)V(z) = NV$. This means that the evolution of $N(z)$ through the space $z \geq 0$ is given by

$$N(\zeta) = \frac{N}{1 + \zeta + \zeta N^2}, \tag{20}$$

where ζ replaces z/R, a dimensionless relative position. The ratio $V(\zeta)/V$ is evaluated from Eq. (6) after replacing θ_0^2 with $\theta_c^2(1 + N^2)$, using Eqs. (6) and (13) to simplify the result. The focusing parameter is a value to determine the position of the geometric focus. We are interested in N since it sets the focusing properties of the region of interest, $\zeta \geq 0$, and is defined by setting Eq. (18) at $z = 0$. The version of N we propose is different from that shown in Ref. [7] in that it includes the beam quality factor. The relationship with M^2 shows that loss of beam quality results in the drop in the value of N except when $V = 0$ that is when the waist is at Y. The process optics are meant to control N so that the beam moments at Y, and in subsequent planes, have the desired values. The parameter to be controlled is V by manipulating the $ABCD$ elements of the process optics. As an example, we select what may be the simplest optical device: a positive thin lens attached directly to the laser source. In that case, N takes the form of $2M^2 f/k(-\omega_i^2 + fV_i)$, expressed in terms of the source parameters. If $V_i = 0$, as in the case of most off-the-shelf laser systems, then N takes on the value $-2M^2 f/k\omega_i^2$ which has a directly proportional relationship with f. Therefore, the control parameter in this particular case is f, with N being the output.

b. Evolution of the normalized local and curvature divergences

From the results so far, the evolution of the divergences as shown in Eqs. (12) and (13) can be presented in terms of N. The results, expressed as normalized by θ_0^2, are as follows:

$$\frac{\theta_l^2(\zeta)}{\theta_0^2} = \frac{N^2}{1 + N^2}\frac{1}{(1 + \zeta)^2 + \zeta^2 N^2}. \tag{21}$$

$$\frac{\theta_c^2(\zeta)}{\theta_0^2} = \frac{1}{1+N^2}\frac{(1+\zeta+\zeta N^2)^2}{(1+\zeta)^2+\zeta^2 N^2}. \tag{22}$$

The two expressions as functions of ζ and N are plotted in Figs. 3(a) and 3(b), respectively. The above equations confirm the fact that the ratios $\theta_l^2(\zeta)/\theta_0^2$ and $\theta_c^2(\zeta)/\theta_0^2$ have values between 0 and 1 and that they add up to 1. In Fig. 3(a), at large $|\zeta|$, $\theta_l(\zeta)$ approaches 0 for all N. There is one value for each N in which $\theta_l(\zeta) = \theta_0$ and they are all located in the range $-1 \le \zeta \le 0$. At large $|N|$, this maximum occurs when $\zeta = 0$. Getting close to $|N| = 0$, the maximum shifts towards, and is ultimately located at, $\zeta = -1$ when $N = 0$, a point we will refer to as x. In Fig. 3(b), the opposite occurs in that $\theta_c(\zeta)$ approaches θ_0 for large $|\zeta|$. The minima in Fig. 3(b) are located in exactly the same coordinates as the maxima of Fig. 3(a). It is apparent that at these maxima/minima, $\zeta = \zeta_0$, the waist location, which is found by calculating the gradient of either Eqs. 3(a) and 3(b), and equating the result to 0. The result is the first equation below:

$$\zeta_0 = -\frac{1}{1+N^2} = -\frac{\theta_c^2}{\theta_0^2};\quad \frac{\omega_0^2}{\omega^2} = \frac{N^2}{1+N^2} = \frac{\theta_l^2}{\theta_0^2} \tag{23}$$

This is sometimes referred to as the relative focal shift of an optical system [4]. It illustrates the relationship between the waist location and the focus and always fulfils the condition, $-1 \le \zeta_0 \le 0$, indicating the limit to which the waist can be located given the field radius of curvature of a focusing beam. The moduli of the focal shift and field curvature are equal only when $N = 0$, i.e., when the waist is at the source or $\zeta_0 \cong -1$, which is in the geometric limit. At any other plane, $\zeta_0 < -1$ for all values of N, that is, the waist is always located before the geometric focus. The second equation is the relative waist size and can be derived by using the definition of the beam parameter product $\omega^2\theta_0^2 - V^2$ in Eq. (9) and expressing the result in terms of $\theta_l(\zeta)$ and $\theta_c(\zeta)$ and finally in terms of N. The waist has limits, $0 < \omega_0 \le \omega$, with a minimum approached at the geometric limit. At $|N| = 0$, the waist width approaches 0. Moreover, we can ascertain an implicit relationship between the two, $\omega_0^2/\omega^2 - \zeta_0 = 1$ by adding the square of the relative local and curvature divergences. This equation gives a mathematical relationship that quantifies the way in which an increase in ω_0 results in an increase in ζ_0 given a specific value of ω.

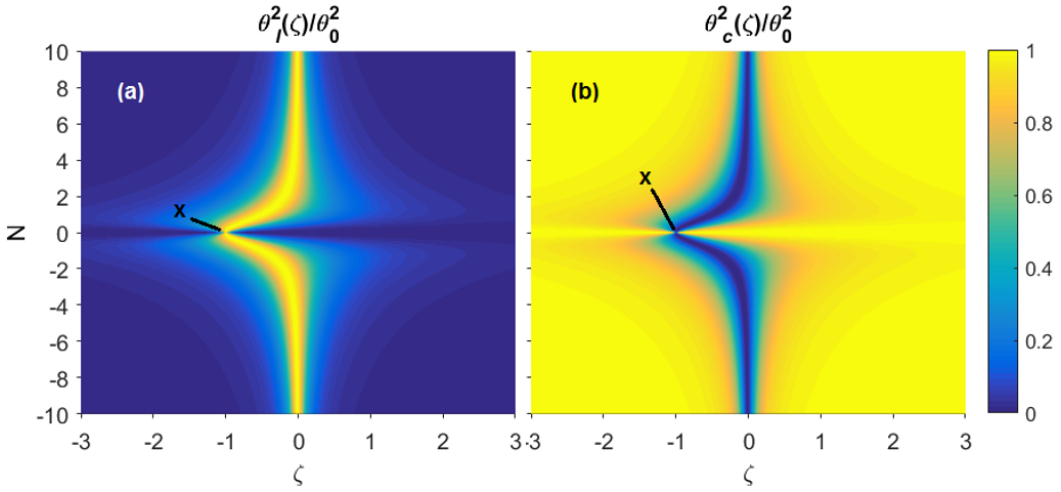

Fig. 3 Local (a) and curvature (b) divergence normalised by the far-field divergence expressed as a function of ζ and N. The point marked x indicates the geometric limit where $(N, \zeta, \theta_l(\zeta)/\theta_o)$ and $(N, \zeta, \theta_c(\zeta)/\theta_o)$ take on values $(0, -1, 1)$ and $(0, -1, 0)$, respectively.

4. Parametric characterization of the paraxial propagation of light beams

For first order beam propagation, we consider the beam during translation where $z \ge 0$. We are in a position to select the conditions at $z = 0$ such that the beam would have selected properties at any point after that. This is achieved by specifying an appropriate $ABCD$ system. It has been established in the previous section that the control parameter would be the focusing parameter, N. To that effect, we need to specify the relationship between various output parameters and N. This allows the system designer to anticipate these parameters by setting N, which can be demonstrated by replacing the lens with one having a different focal length. At the very least, we intend to use this model to analyse the limits of the parameters that can be acquired given certain input beam conditions. Including N in the model allows the inclusion of the local and curvature divergences where we use Eqs. (19), (21) and (22) to make the necessary changes.

We begin with the beam width as defined by Eq. (2). In this case, the equation is normalised by the beam width, which simplifies the result. Expressed in terms of the focusing parameter, we get

$$\frac{\omega^2(\zeta)}{\omega^2} = (1+\zeta)^2 + \zeta^2 N^2 = \frac{\theta_l^2}{\theta_l^2(\zeta)}. \tag{24}$$

The third term comes from combining Eq. (21) and the second equation of Eq. (23). The propagation invariant, $\omega(\zeta)\theta_l(\zeta)$, can also be utilized to make the same connection. The graph for Eq. (24) is shown in Fig. 4. As expected, $\omega(\zeta)$ increases with increase in $|N|$. In other words, the smaller $|N|$ is, the more focused the beam. The point $\zeta = 0$ is the starting point of the beam propagation, with positive values (when $R > 0$) indicating a diverging beam. Negative values (when $R < 0$) indicate a converging beam to a Gaussian plane at $\zeta = -1$, whose beam width is given by $\omega_f = \omega(-1) = N\omega$. The size of the beam has a minimum relative value at $(-1/(1+N^2); N^2/(1+N^2))$ which is identical to $(\zeta_0; \omega_0^2/\omega^2)$ and $(-\theta_c^2/\theta_0^2; \theta_l^2/\theta_0^2)$. This means that it varies between 0 and 1 at the points where ζ is between -1 and 0. In the geometric limit the minimum is at $\{-1; 0\}$ and the graph follows the equation $\omega(\zeta)/\omega = |1+\zeta|$, which is symmetric about $\zeta = -1$, as the term in the centre becomes very small. In other words, only in the geometric limit is the waist location the same as the Gaussian plane. At any other N, the waist location falls short of the Gaussian plane. The larger N is, the further the waist is removed from the Gaussian plane. In the other extreme, when $N \to 0$ the minimum tends to 1 and we get $\omega(\zeta)/\omega \cong N\zeta$ as a result of the central term becoming very large. In the process, the graph becomes more symmetrical about the vertical axis, meaning that the waist remains at the initial position. The graph of $\theta_l(\zeta)/\theta_l$ is shown in Fig. 4(b) which is in fact a reciprocal of Fig. 4(a) which means that the minima of each graph becomes the maxima. At $N = 0$, the local divergence magnification is infinite meaning that it is undefined in the geometric limit. For all N and $\zeta = 0$, $\theta_l(\zeta) = \theta_l$ which means that $\theta_l(\zeta)$ remains constant. For large $|N|$, the maxima is located at $\zeta = 0$ but as $|N|$ approaches 0, the maxima at each N, $\theta_l(\zeta) > \theta_l$, and $|\zeta|$ slowly shifts towards the point at which $\theta_l(\zeta)/\theta_l$ approaches ∞.

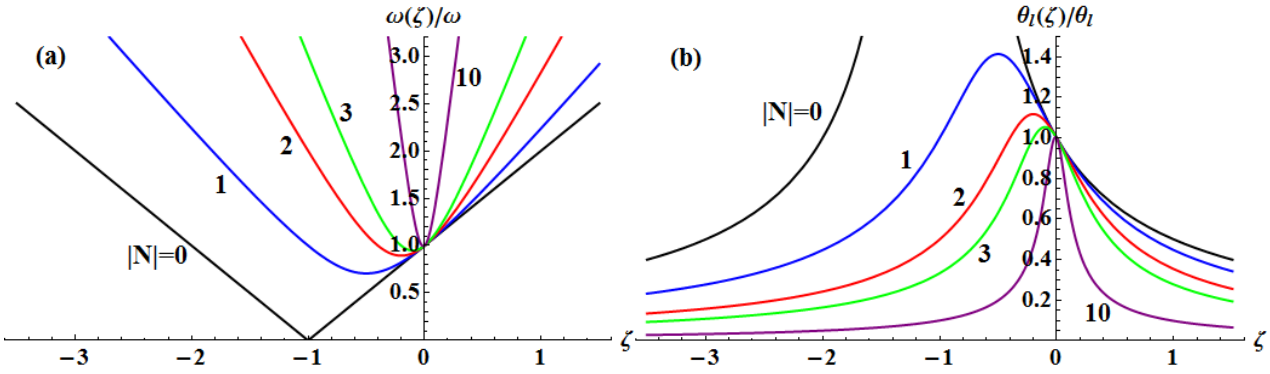

Fig. 4 Beam size (a) and local divergence (b) magnifications as functions of the relative position at selected values of N.

The normalized space-angular moment derived from Eq. (20), is given by

$$\frac{V(\zeta)}{V} = 1 + \zeta + \zeta N^2 = \frac{N}{N(\zeta)}. \tag{25}$$

The plot of $V(\zeta)/V$ versus ζ shown in Fig. 5(a) is a straight line of gradient $1 + N^2$ with the intercept at 1 for all N. The graph crosses the horizontal axis when ζ takes a value of $-1/(1+N^2)$ which is the relative waist location (see Eq. (23)). Since N varies from 0 to ∞ the intercept on this axis will be between -1 and 0 for all values of N. The gradient of each graph is θ_0^2/θ_c^2 and varies between 1, at the geometric limit, and ∞, a vertical line also passing through the origin. The condition $V(\zeta) = 0$ is fulfilled when ζ has the same value as the minima of Fig. 4(a), namely $-\theta_c^2/\theta_0^2$. This agrees with the space-angular moment being zero when the size of the beam is smallest at its waist. The last term of Eq. (25) is plotted in Fig. 5(b). The asymptotes of this graph are obviously located at points where the graphs of Fig. 5(a) cross the horizontal axis and are all located between 0 and -1.

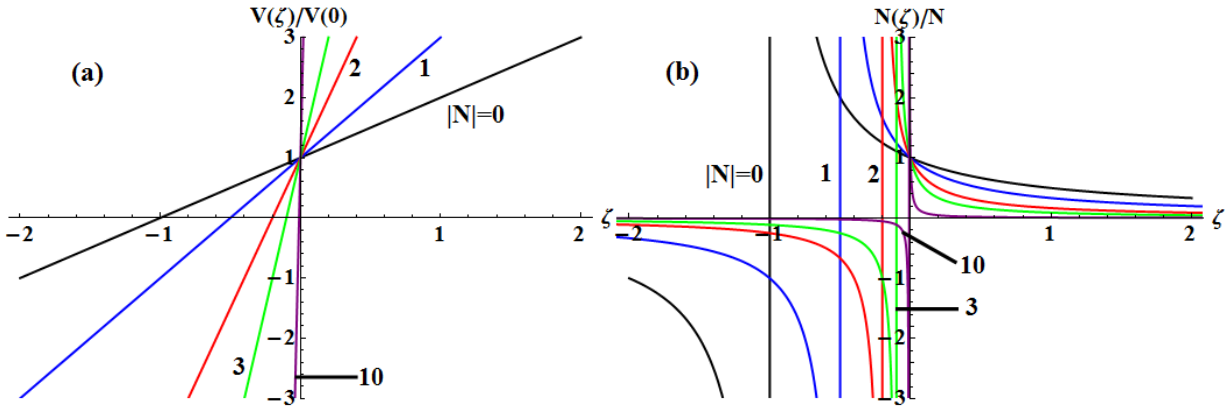

Fig. 5 Space-angular moment (a) and focusing parameter (b) as magnifications as functions of the relative position at selected values of N.

The evolution of the curvature divergence can be calculated from combining Eq. (22) with the first equation of Eq. (23) which results in the first equation below;

$$\frac{\theta_c^2(\zeta)}{\theta_c^2} = \frac{(1+\zeta+\zeta N^2)^2}{(1+\zeta)^2+\zeta^2 N^2} = \frac{R^2}{R^2(\zeta)}. \tag{25}$$

The equation is plotted in Fig. 6(a) and shows a trivial result that when $N = 0$, $\theta_c(\zeta) = \theta_c$ for all ζ except at $\zeta = -1$ where it approaches 0 as $|N| \to 0$. For each $|N| \neq 0$, the relationship between $\theta_c(\zeta)/\theta_c$ versus ζ possesses a minimum which match the maxima of Fig. 3(a). For large $|N|$, this minima has a value $\theta_c(\zeta) = 0$, that is, when $\zeta = 0$ but as $|N| \to 0$, $\theta_c(\zeta) \to \theta_c$ until it reaches this mark when $N = 0$ and $\zeta = -1$ which is the geometric limit. In the limit, $\zeta \to \pm\infty$, $\theta_c(\zeta)/\theta_c \to \sqrt{1+N^2}$ for all N. Also note that when $\zeta = 0$, $\theta_c(\zeta) = \theta_c$ for all N. The second term of the above equation can be simplified by replacing the numerator and denominator by Eqs. (25) and (24), respectively where they are expressed in terms of the subject terms, respectively. The result is $(V(\zeta)/V)^2/(\omega/\omega(\zeta))^2$ which, when simplified using Eq. (7) reduces to the right hand side of Eq. (25). This gives an expression of the evolution of the radius of curvature which is the reciprocal of the evolution of the curvature divergence. As a result, it is plotted in Fig. 6(b) and shows that the minima acquired in Fig. 6(a) translate to asymptotes when the initial wavefront is flat, that is, when curvature, $1/R = 0$. Note that Eq. (25) translates into yet another propagation invariant, $\theta_c(\zeta)R(\zeta) = \theta_c R$.

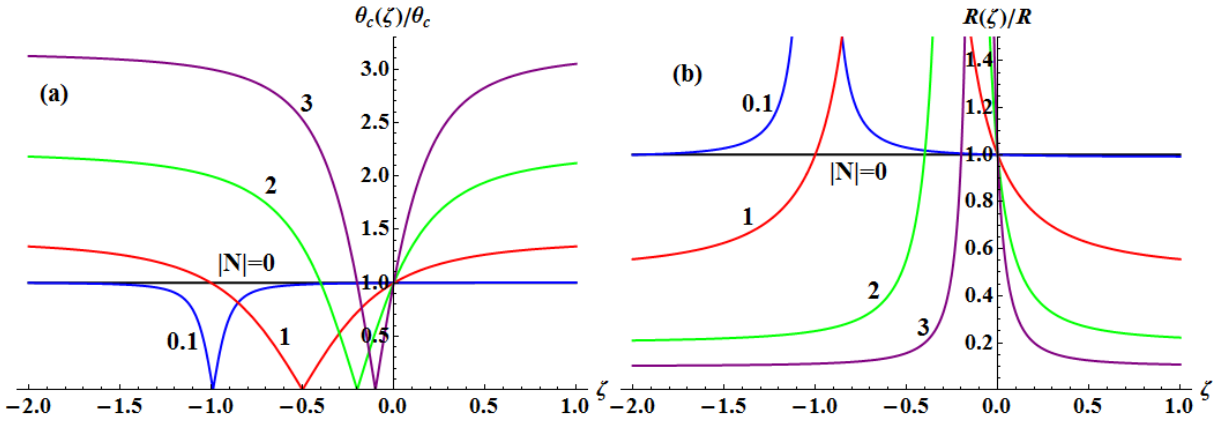

Fig. 6 Curvature divergence (a) and wavefront radius of curvature (b) magnification as functions of the relative position at selected values of N.

We can look at the Rayleigh planes, $\zeta_\pm$, calculated from the expression Eq. 11. The resultant equation is given by

$$\zeta_\pm = \frac{-1 \pm N}{1+N^2} = \frac{-\theta_c^2 \pm \theta_c\theta_l}{\theta_0^2};\ -\frac{1}{2}-\frac{1}{\sqrt{2}} \le \zeta_\pm \le -\frac{1}{2}+\frac{1}{\sqrt{2}}. \tag{26}$$

Plots of ζ_+ and ζ_- are illustrated in Fig. 7. The results clearly show that there is a maximum limit beyond which the relative position of the Rayleigh planes cannot be located given the radius of curvature, R. The output fits in the range given on the right hand side of Eq. (26). This implies that the ζ_+ curve has respective maxima and minima at points, $\{1+\sqrt{2}, -1/2 + 1/\sqrt{2}\}$ and $\{1-\sqrt{2}, -1/2 - 1/\sqrt{2})\}$ and the ζ_- curve has maxima and minima at $\{-1-\sqrt{2}, -1/2 + 1/\sqrt{2}\}$ and $\{-1+\sqrt{2}, -1/2 - 1/\sqrt{2}\}$, respectively. In the limit of large $|N|$, $\zeta_\pm$ approaches 0, and at the geometric limit, both graphs coincide at the point $(0, -1)$ where $\zeta_R = 0$. The section of the graph below the horizontal axis represents a focused beam and shows that the limit of $\zeta_\pm$ is $-1/2 - 1/\sqrt{2}$ where $N = -1+\sqrt{2}$ and $1-\sqrt{2}$ for ζ_- and ζ_+, respectively. The section above the horizontal axis corresponds to a diverging beam having a limit of $-1/2 + 1/\sqrt{2}$ where $N = 1+\sqrt{2}$ and $-1-\sqrt{2}$ for ζ_+ and ζ_-, respectively. The Rayleigh range normalized by the radius of curvature in terms of N is shown to be

$$\zeta_R = \frac{N}{1+N^2} = \frac{\theta_l\theta_c}{\theta_0^2};\ -\frac{1}{2} \le \zeta_R \le \frac{1}{2}. \tag{27}$$

It is apparent that ζ_R has a modulus less than 0.5, meaning that for any beam, the maximum Rayleigh range that can be achieved is half the radius of curvature at $\zeta = 0$, regardless whether the beam is focused or diverging. The graph for Eq. (27) is shown in Fig. (6) as well and calculated at each N using the expression $(\zeta_+ - \zeta_-)/2$. This result is responsible for setting the range of the product of the local and curvature divergences between -0.5 and 0.5 of the far-field divergence squared, which is achieved when $N = -1$ and 1, respectively.

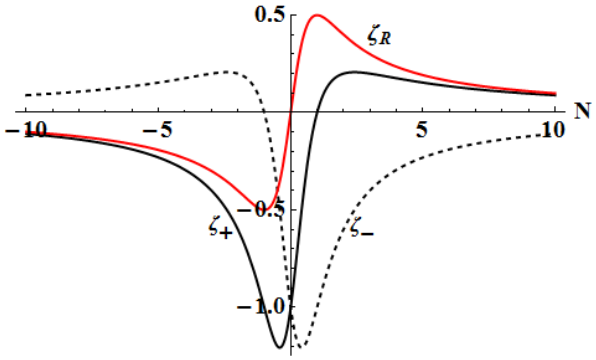

Fig. 7 Normalised Rayleigh planes as a function of the focusing parameter, N.

5. Discussion and conclusion

The model we have presented allows for the complete characterization of any light beam in which any of the three second order moments, width, divergence and space-angular moment, can be acquired from the measured electric field through calculation. The measurements are expected to take place in one plane assuming that the projected propagation is paraxial and through free space such that other parameters such as waist width and location, divergence, Rayleigh range and field curvature, can be calculated from the second order moments. We have already shown how the measurement of M^2 can be so acquired. For this discussion, we assumed that we are starting our calculation at $z = 0$ where we obtain ω, θ_0 and V and consequently also M^2. From Eqs. (7), (8), (9) and (11), we can calculate R, z_0, ω_0 and z_R, respectively. The value of $\omega(z)$, $V(z)$ at some plane $z > 0$ can be calculated using the appropriate form of Eqs. (2) and (4), from which $R(z)$ is calculated using Eq. (7). The changes that the beam would go through if the translation is replaced by a generalized $ABCD$ system can be realised again using Eqs (2)-(4). We have also shown parameters - the local divergence, an established but relatively unknown parameter, and curvature divergence, a new parameter – both which can be calculated from the basic parameters as shown in Eqs. (12) and (13). We have established that the squares of these two divergences add up to the far-field divergence squared.

We have rewritten the beam propagation theory by expressing all the important parameters in normalized form in which the focusing parameter N was introduced. The analysis allowed us to look further, investigate the limits of the various parameters under various conditions. Though aspects of this work has been demonstrated in a previous publication [4] including the references mentioned therein, we showed, in a new result, that the focusing parameter can be defined as a ratio of the local to curvature divergence. This allowed us to replace the focusing parameter with the divergences in order to study them in relation to other propagation parameters such as beam width, space-angular moment, waist width and location, and Rayleigh range. The normalized nature of the formulation allows the user to compare two beams under different propagation regimes. A typical example is a high power continuous wave laser beam that can be scaled up to several kilowatts. Most of these systems are fitted a transmission system which includes a collimator to keep the far-field divergence as low as possible and a window is usually fitted to a collimator to limit the contamination of the system. However, as one scales up the power, the window and, to some extent, the collimator experience thermal lensing. This means that the transmitted beam experiences focusing, which causes it to get smaller at the target as the power is scaled up. It would be prudent to determine the focusing parameter at each power scale at which each measurement is taken as a way of quantifying the thermal effect of the laser system on the transmission systems or a particular component. The process can be repeated every time a new component is added onto the propagation path of the high power beam. Once the focusing parameter is determined, it becomes easier to better predict and simulate the performance of the whole system.

We also discussed the following six propagation invariants: $\omega_0\theta_0$, $\omega(z)\theta_l(z)$, $z_R\theta_0^2$, $N(z)V(z)$, $\theta_c(z)R(z)$ and ω_0^2/z_R. Since the first five invariants are expressed as products of two parameters, increasing one parameter by a certain factor reduces the other one by the same factor. In theory, if one wants to increase ω_0 to such an extent that it can capture the beam profile at the waist, then one should decrease θ_0 by an appropriate preselected factor. The sixth invariant is expressed as a ratio, which means that both ω_0^2 and z_R increase or decrease by the same factor. Since all the invariants are all equal to $2M^2/k$, individually, they can be used to determine M^2. Moreover, they can be equated to each other to solve for any unknown.

References

1. P. A. Belanger, Opt. Lett., Beam propagation and the ABCD ray matrices 16, 4 (1991).
2. M. A. Porras, J. Alda, and E. Bernabeu, Complex beam parameter and ABCD law for non-Gaussian and nonspherical light beams, Appl. Opt, 31, 30 (1992).
3. J. Alda, J. Alonso & E. Bernabeu, "Characterization of aberrated beams," J. Opt. Soc. Am. A 14, 2737-2747 (1997).
4. C. Mafusire & A. Forbes, "Generalized beam quality factor of aberrated truncated Gaussian laser beams," J. Opt. Soc. Am. A 28, 1372-1378 (2011).
5. C. Mafusire & A. Forbes, "Mean focal length of an aberrated lens," J. Opt. Soc. Am. A 28, 1403-1409 (2011).
6. International Standards Organization, Lasers and laser-related equipment; Test methods for laser beam widths, divergence angle and beam propagation ratio, ISO 11146-1 Part 1: Stigmatic and simple astigmatic beams, 2005-02-15.
7. L. C. Andrews, W. B. Miller, and J. C. Ricklin, Geometrical representation of Gaussian beams propagating through complex paraxial optical systems, Appl. Opt., 32, 30 (1993)

8. D. R. Neal, J. K. Gruetzner, and J.P. Roller, Use of beam parameters in optical component testing, Optical Manufacturing and Testing IV, H. Philip Stahl, Editor, Proceedings of SPIE Vol. 4451 (2001)